

Anomalous magnetoentropic response of skyrmion crystals

Ahmed R. Saikia¹ and Narayan Mohanta^{1,*}

¹*Department of Physics, Indian Institute of Technology Roorkee, Roorkee 247667, India*

We investigate theoretically magnetoentropic signatures of the crystal phase of magnetic skyrmions of various kinds, commonly appearing in two dimensions, *viz.*, Néel, Bloch and anti skyrmions. Using Monte Carlo calculations based on spin Hamiltonians, we obtain magnetic entropy change ΔS_m in the presence of three different types of Dzyaloshinskii-Moriya interactions responsible for these skyrmions. The phase mapping of ΔS_m using skyrmion counting number N_{sk} in temperature-magnetic field plane reveals fluctuation-dominated weak first-order transition in the precursor phase of the skyrmions, and a sign change in ΔS_m when the system enters into the skyrmion crystal phase—in agreement with recent experimental findings. We also find that the fractional entropy change in going from a ferromagnetic phase to the skyrmion crystal phase is much larger compared to the conventional route of paramagnetic phase to ferromagnetic phase, used for the purpose of magnetic cooling. The magnetoentropic signatures of the different types of skyrmion crystals are found to be similar. Our results indicate that the skyrmion crystals exhibit enhanced cooling efficiency and have the potential to upgrade the existing magnetic cooling methods.

I. INTRODUCTION

Chiral spin fluctuations in magnets with antisymmetric Dzyaloshinskii-Moriya interaction (DMI) near the onset of magnetically ordered phases give rise to anomalies in various physical observables including magnetization, specific heat, electric polarization and magnetic susceptibility [1–3]. These chiral spin fluctuations, driven primarily by the frustration introduced by the DMI and aided by intrinsic inhomogeneities, also generate strong signatures in the magnetic entropy near the temperature-driven transition to the ordered phases. In chiral magnets and spinel compounds, which support skyrmion crystal (SkX) phase at high temperatures, the magnetic entropy response was found to clearly distinguish the SkX phase from other topologically trivial phases such as conical and ferromagnetic phases [4–9]. The SkX phase appears also robustly in two dimensions, at the interface between two oxide compounds and in van der Waals magnets, stabilized by a magnetic anisotropy which originates from interfacial strain and favors the long-range magnetic order [10–18]. Within a range of temperatures above the critical temperature for the SkX phase, the average scalar spin chirality $\chi = \langle \mathbf{S}_i \cdot (\mathbf{S}_j \times \mathbf{S}_k) \rangle$ can be finite even when $\langle \mathbf{S}_i \rangle \approx 0$. The nature of the phase transition from the paramagnetic phase to the SkX phase is, therefore, dictated primarily by the spin chirality fluctuation.

In this paper, we investigate the behavior of the magnetic entropy as the transition to the SkX phase takes place in two dimensional magnets, and explore the classification strategy of the SkX phase using the magnetoentropic response. The central object of our investigation is the magnetic entropy change, which can be obtained using the following Maxwell's thermodynamics relation

$$\left(\frac{\partial S}{\partial H} \right)_T = \left(\frac{\partial M}{\partial T} \right)_H \quad (1)$$

The above relation provides the magnetic entropy change ΔS_m in terms of the temperature dependence of magnetization. We perform Monte Carlo calculations and obtain ΔS_m as a function of temperature and magnetic field, and obtain the magnetoentropic response of various ordered phases. Magnetic skyrmions are topologically stable spin texture which can be characterized by an invariant known as the skyrmion number, defined as

$$N_{sk} = \frac{1}{4\pi} \int \mathbf{S} \cdot \left(\frac{\partial \mathbf{S}}{\partial x} \times \frac{\partial \mathbf{S}}{\partial y} \right) dx dy. \quad (2)$$

The SkX phase exhibits a large value of N_{sk} ; hence it provides an useful tool to map out the SkX phase by comparing N_{sk} with ΔS_m in the phase plane spanned by magnetic field and temperature. We perform this magnetoentropic mapping for three different types of DMI in two dimensions which give rise to three common types of skyrmions, *viz.*, Néel, Bloch and anti skyrmions. Besides, ΔS_m can also shed light on the puzzle in understanding the role of critical spin fluctuations as the system transitions to the SkX phase when the temperature is lowered. The puzzle arises because specific heat measurements reveal a first-order transition at zero magnetic field to the helical state [19], while neutron probes reveal Landau soft-mode mechanism of weak crystallization to the SkX phase at finite magnetic fields [20–22]. These experimental observations suggest that phase transitions in Dzyaloshinskii-Moriya magnets occur via a precursor phase in which chiral spin textures emerge with an abundance of spin fluctuations. The magnetic entropy change ΔS_m can provide a great amount of information about the fluctuation-induced gradual first-order transition to the SkX phase [23]. Valleys and peaks in ΔS_m can reveal phase transitions which can be detected in experiments and give information complementary to the conventional signatures in the heat capacity $C = T(\partial S / \partial T)$ [8]. We find that for all three types of skyrmions, there is a change in the slope in the temperature variation of ΔS_m as the system enters into the precursor phase from the spin-disordered paramagnetic phase. Also, ΔS_m under-

* narayan.mohanta@ph.iitr.ac.in

goes a change in sign as the system enters the fully-ordered SkX phase. These features enable us to identify the critical temperatures for the precursor phase and the fully-ordered SkX phase. The magnetic entropy change can also provide valuable insights into entropy-limited topological protection and lifetime of skyrmions [24].

Conventional magnetic alloy compounds exhibiting a large magnetic entropy change also suffer from considerable thermal hysteresis effect which makes these materials unsuitable for applications in refrigerators due to their low performance in the cyclic operation at high cycle frequencies [25]. The irreversibility of the magnetization also causes serious problems in estimating the magnetocaloric effect from the magnetization measurements [26–28]. We here also discuss about magnetic cooling efficiency of a cooling cycle involving a SkX phase, and compare it qualitatively with the conventional cycle involving the paramagnetic and ferromagnetic phases. Based on our estimation of a large fractional entropy change, we propose that the cyclic route between the ferromagnetic phase and the SkX phase can enable a more efficient magnetic cooling method. Compounds hosting topological spin textures such as the SkX can, therefore, be a promising alternative for the refrigeration applications with high efficiency.

The remainder of this paper is organized as follows: in section II, we discuss our theoretical model and provide details of our Monte Carlo annealing simulation. In section III, we present the numerical results of the magnetic entropy change ΔS_m as the temperature is reduced while approaching various phases *viz.* spin spiral (SS), SkX and ferromagnetic (FM) phases, all stabilized at low temperatures in our considered two-dimensional spin systems. In section III, we discuss the experimental relevance of our results, enhanced magnetic cooling efficiency of the SkX phase, and summarize our results.

II. MODEL AND METHOD

We consider two-dimensional spin systems with competing Heisenberg exchange interaction and DMI, in the presence of an external magnetic field applied perpendicular to the two-dimensional plane (considered to be the x - y plane) and an easy-plane magnetic anisotropy. The model Hamiltonian for such systems is given by

$$\mathcal{H} = -J \sum_{\langle ij \rangle} \mathbf{S}_i \cdot \mathbf{S}_j + \mathcal{H}_{\text{DMI}} - H_z \sum_i S_{zi} - A \sum_i |S_{zi}|^2 \quad (3)$$

where $\mathbf{S}_i \equiv (S_{xi}, S_{yi}, S_{zi})$ represents the spin vector of magnitude $S = 1$ at site i , J is the strength of nearest-neighbor Heisenberg exchange interaction, \mathcal{H}_{DMI} is the Hamiltonian describing the DMI which is mentioned below, H_z is the strength of the perpendicular magnetic field, and A is the easy-plane magnetic anisotropy which helps to stabilize the magnetic skyrmions and the long-range order in the SkX [29–32]. We used $A = 0.001J$

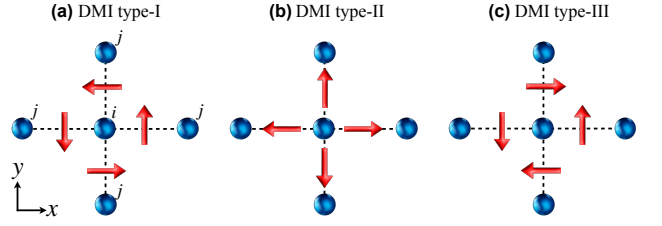


FIG. 1. Schematic representation of the three types of Dzyaloshinskii-Moriya interaction (DMI) considered in the two-dimensional geometry. Blue spheres represent nearest-neighbor lattice sites, with indices i and j . Red arrows denote the vectors of the DMI in the three cases, which give rise to (a) Néel, (b) Bloch and (c) anti skyrmions, respectively.

throughout this paper.

As discussed widely in literature, the DMI term is relevant in materials with strong spin-orbit coupling and broken inversion symmetry. Magnets with sizeable Rashba spin-orbit coupling, such as those interfacing another compound in a two-dimensional plane, are candidate systems where the DMI amplitude is typically large. Here we consider three different types of DMI, commonly appearing in two dimensions and responsible for the Néel, Bloch and anti skyrmions. The vectors representing these three types of DMIs are shown in Fig. 1, and the explicit forms of \mathcal{H}_{DMI} in these three cases are expressed as

$$\mathcal{H}_{\text{DMI}} = -D \sum_{\langle ij \rangle} (\hat{z} \times \hat{r}_{ij}) \cdot (\mathbf{S}_i \times \mathbf{S}_j), \quad (4)$$

$$\mathcal{H}_{\text{DMI}} = -D \sum_{\langle ij \rangle, \hat{e}=\hat{x}, \hat{y}} (\pm \hat{e}) \cdot (\mathbf{S}_i \times \mathbf{S}_{j=i \pm \hat{e}}), \quad (5)$$

$$\mathcal{H}_{\text{DMI}} = -D \sum_{\langle ij \rangle} \eta (\hat{z} \times \hat{r}_{ij}) \cdot (\mathbf{S}_i \times \mathbf{S}_j), \quad (6)$$

where, in the last expression $\eta = +1$ for $j = i \pm \hat{x}$ and $\eta = -1$ for $j = i \pm \hat{y}$. The DMI in Eq.(4), Eq.(5) and Eq.(6) stabilizes, respectively, the Néel, Bloch and anti skyrmions in two dimensional lattices. We consider $J = 1$, and express all other energies in units of J .

The SkX phase can also originate without the explicit need of the DMI or external magnetic field, from spin frustration or interfacial phase frustration [33–35]. We anticipate our discussions below and the magnetoentropic signatures to be relevant in those unconventional SkXs as well.

Monte Carlo annealing: Spin configurations are obtained using Monte Carlo (MC) annealing procedure on a square lattice of size 24×24 with open boundary conditions. The annealing process was started at a high temperature $T = 10J$ with an initial random spin configuration, and the temperature was gradually lowered down to $T = 0.001J$ in 500 steps. At each temperature step, 10^8 MC spin update steps are performed. At each spin update step, a new direction of the spin vector at a randomly-selected site is chosen randomly within a small cone of angle $\Delta\theta = 2^\circ$ around the initial spin direction.

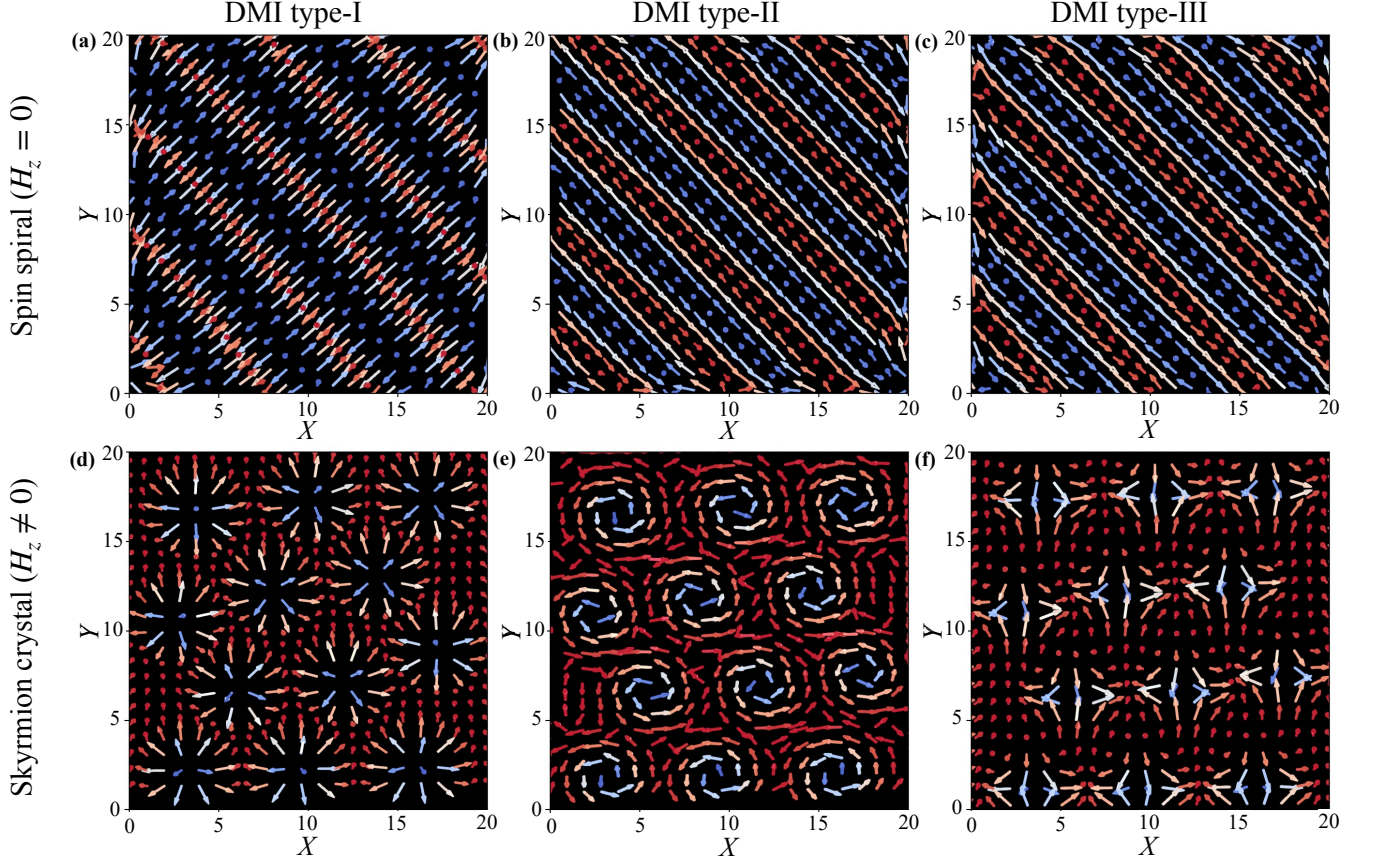


FIG. 2. Spin configurations in the spin spiral (SS) and the skyrmion crystal (SkX) phases, obtained in Monte Carlo annealing process at a low temperature $T=0.001J$ on a 24×24 square lattice with periodic boundary conditions. (a), (b), (c) SS texture realized in the absence of any magnetic field (*i.e.* at $H_z = 0$) for the three types of DMI discussed in Sec. II. (d), (e), (f) Triangular crystal structure of Néel, Bloch and anti skyrmions, respectively, obtained at a magnetic field $H_z = 1.8J$. The colors in the arrows represent the z component of the spin vector, blue (red) being the down (up) spin arrangement. Other parameters used are $J=1$, $D=0.5J$, and $A=0.001J$.

The new *trial* spin configuration is accepted or rejected using the standard metropolis algorithm: accepted if the energy difference ΔE between the two spin configurations is negative, and accepted with the Boltzmann probability $e^{-\Delta E/(k_B T)}$ when ΔE is positive; the latter is to incorporate the thermal spin fluctuation which increases with temperature.

Calculation of magnetic entropy change: The change in the magnetic entropy at a given temperature T and magnetic field H is obtained, using Eq. (1), as

$$\Delta S_m(H, T) = \frac{\mu_0}{T_2 - T_1} \int_0^H M(T_2, H) - M(T_1, H) dH \quad (7)$$

where, $T_1 = T - \Delta T$, $T_2 = T + \Delta T$ are two considered temperatures around T , ΔT is incremental temperature gradient, μ_0 is the free-space permeability, and M is the average magnetization. The above integral is evaluated numerically using the Simpson's method from the magnetization data obtained in MC simulations. To enhance the smoothness of the magnetic entropy variation with T ,

a Savitzky-Golay filter was applied. This filtering scheme uses a 4th order polynomial for local fitting, and reduces high-frequency noise from the entropy signal, revealing a clearer representation of the overall trend in the entropy change.

Calculation of skyrmion number: The skyrmion number in Eq. (2) can be expressed in discretized form as

$$N_{sk} = \frac{1}{4\pi} \sum_{i,j} \mathbf{s}_{ij} \cdot [(\mathbf{s}_{i+1,j} - \mathbf{s}_{i,j}) \times (\mathbf{s}_{i,j+1} - \mathbf{s}_{i,j})], \quad (8)$$

in which the integration in Eq. (2) has been replaced by a summation and the partial derivatives are evaluated using a central-difference scheme. Magnetic skyrmions can be classified by the topological index N_{sk} , since under transformation of the underlying lattice from a torus to a sphere a skyrmion gives a full coverage of the sphere—a unique feature of the topological structure of the skyrmion. The number N_{sk} , therefore, helps in the characterization of the skyrmions, especially the SkX phase, in the phase plane spanned by the magnetic field and temperature.

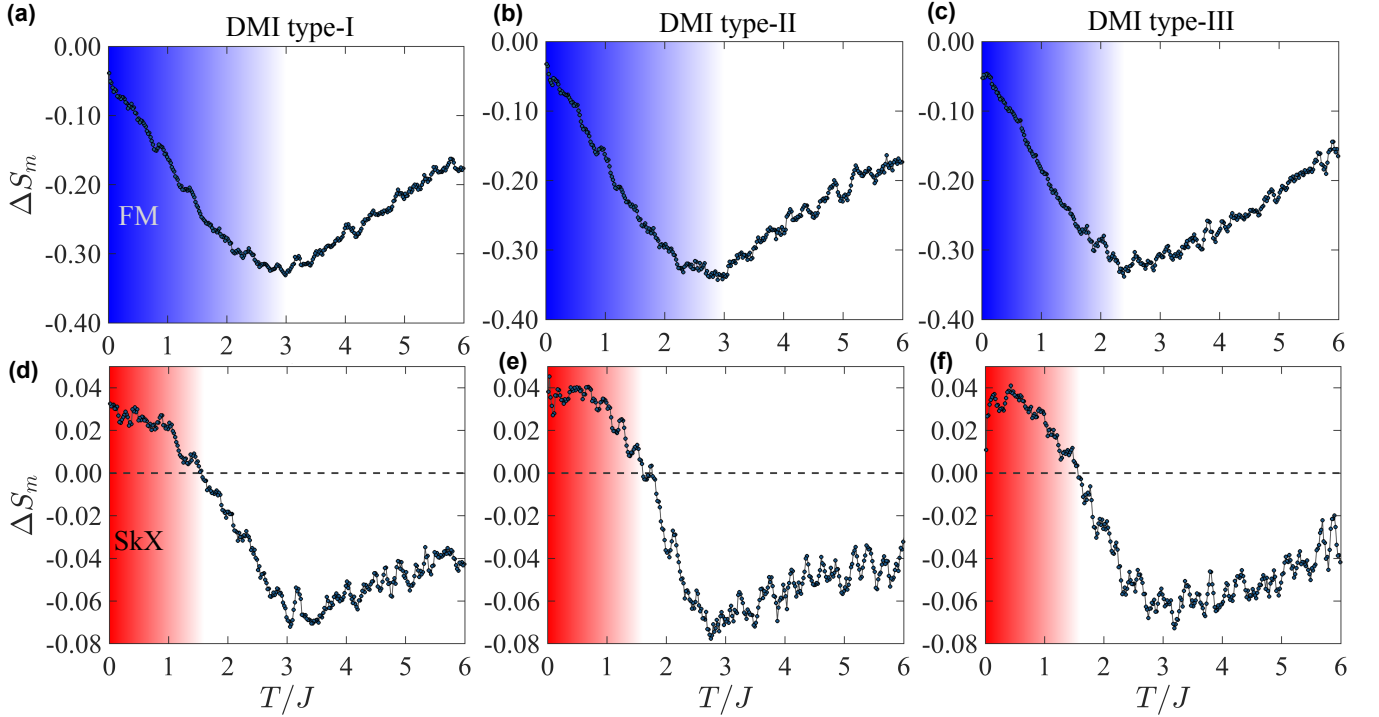


FIG. 3. (a),(b),(c) Temperature variation of magnetic entropy change ΔS_m for the three types of DMI discussed in Sec. II, at a magnetic field $H_z = 4.4J$ which stabilizes the FM phase (blue region) at low temperatures. (d),(e),(f) Temperature variation of ΔS_m for the three types of DMI, at $H_z = 1.8J$ which stabilizes the SkX phase (red region) at low temperatures. Other parameters used are $J = 1$, $D = 0.5J$, and $A = 0.001J$. The upward turn in ΔS_m indicates the entrance to the ordered phase via the fluctuation-dominated regime. The change in the sign of ΔS_m occurs when the skyrmions stabilize and form a triangular crystal at low temperatures.

III. RESULTS

A. Three types of skyrmion crystals

In our two-dimensional spin systems, the SkX phase appears at low temperatures within a range of external magnetic fields, for all three types of DMI described above. The MC-generated spin configurations representing the chiral ordered phases, *viz.* the spin spiral (SS) which appear in the absence of any magnetic field and the SkX, for the three types of DMIs at a low temperature $T = 0.001J$ are shown in Fig. 2. Fig. 2(a),(b),(c) show one of the two natural solutions of diagonal arrangements for the SS configurations. On the other hand, Fig. 2(d),(e),(f) show triangular crystals of Néel, Bloch and anti skyrmions, respectively. Promising platforms in which such two-dimensional skyrmions can appear are interfaces between compounds with competing magnetic interactions and broken inversion symmetry at the interface [10–12, 14–18]. At finite temperatures, the phase boundaries between the SS, the SkX and the fully-polarized FM phases are not sharp, but rather exhibit a region with metastable spin configurations with characteristics of the neighboring phases and governed primarily by thermal fluctuations [17]. One such metastable

phase which is important for the below discussion is the precursor phase of the skyrmions which prevails at temperatures above the critical temperature for the SkX phase.

B. Temperature dependence of entropy change

Fig. 3 shows the temperature dependence of the magnetic entropy change ΔS_m for the three types of DMI discussed in Sec. II and at two values of the magnetic field $H_z = 4.4J$ and $H_z = 1.8J$, at which the system is stabilized in the FM and the SkX phases at low temperatures, respectively, upon cooling from the spin-disordered paramagnetic phase. At $H_z = 4.4J$ (Fig. 3(a),(b),(c)), for which the FM phase is stabilized at low temperatures, the magnitude of ΔS_m is peaked at a critical temperature $T \approx 3J$, at the onset of the FM phase, below which it starts to decrease. A similar behavior is observed at $H_z = 1.8J$, for which the SkX phase is stabilized at low temperatures— ΔS_m shows upturn below a temperature $T \approx 3J$. In addition, in this case ΔS_m changes sign at $T \approx 1.8J$. This positive entropy change is revealed in all three types of the DMI settings.

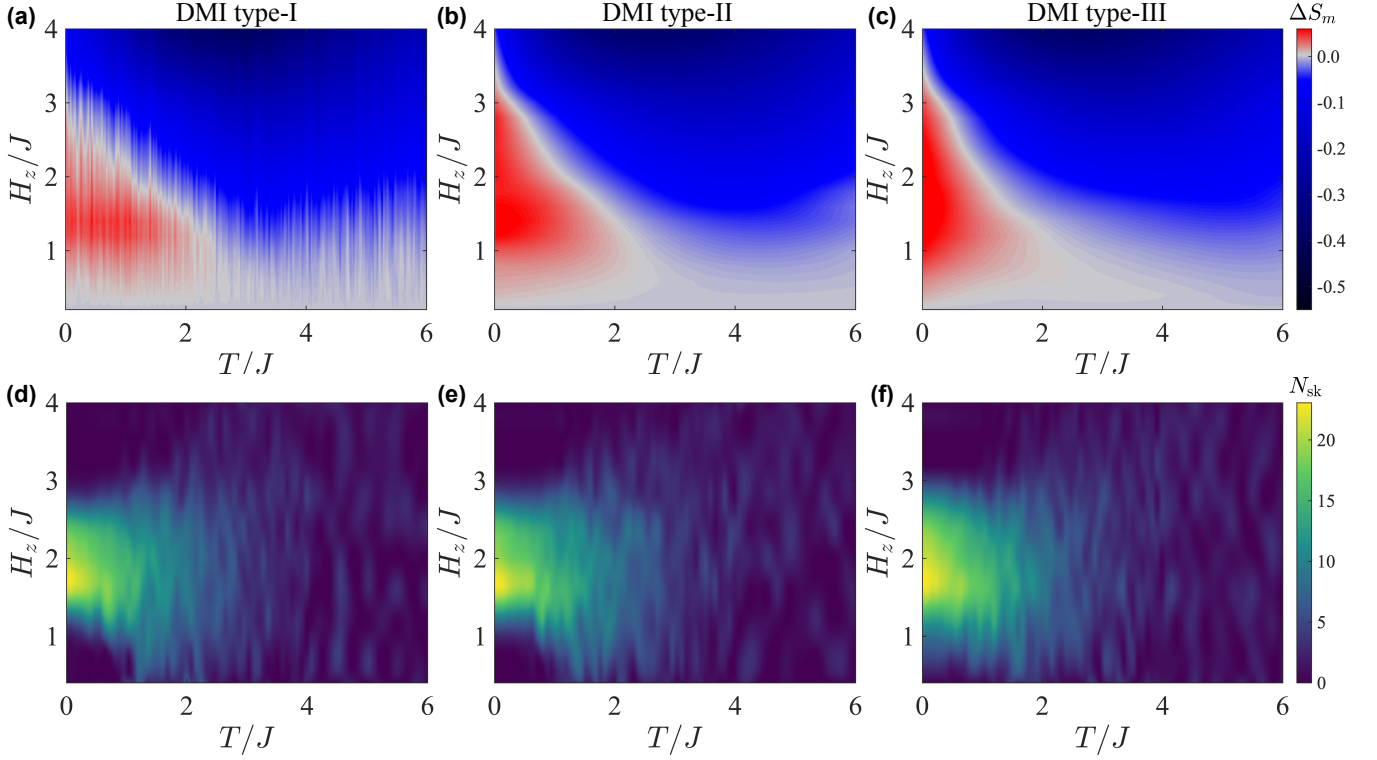


FIG. 4. Magnetic entropic change ΔS_m (top row in (a),(b),(c)) and the skyrmion number N_{sk} (bottom row in (d),(e),(f)) in the temperature T vs. magnetic field H_z plane, for the three types of DMI configurations. The top and bottom rows provide a magnetoentropic mapping of the skyrmion crystal phase—shown by the red regions in top panels and bright yellow regions in below panels. Parameters used are $J=1$, $D=0.5J$, and $A=0.001J$.

C. Entropy response in the skyrmion crystals

To understand the connection between the features in the magnetic entropy change ΔS_m and various temperature dependent phase transitions, we compare ΔS_m with the skyrmion number N_{sk} in the parameter plane spanned by temperature T and the external magnetic field H_z , as shown in Fig. 4. At larger values of the magnetic field ($H_z \gtrsim 3J$), for which the fully-polarized FM phase is stabilized at low temperatures, ΔS_m varies continuously with temperature and exhibits a maximum in its absolute value near the critical temperature for the transition to the FM phase, as shown by the dark blue regions in Fig. 4(a)-(c). At smaller values of the magnetic field ($H_z \lesssim 0.5J$), the transition takes place from the spin-disoriented paramagnetic to the SS phase upon lowering the temperature. In this case, the change in the magnetic entropy is nearly zero, as shown by the white regions in Fig. 4(a)-(c). At intermediate values of the magnetic field ($1.5 \lesssim H_z \lesssim 2.5J$), the SkX phase is stabilized at low temperatures, as evident from Fig. 4(d)-(f). Remarkably, ΔS_m undergoes a sign change as the system enters into the SkX phase either from the paramagnetic phase or from the fully-polarized FM phase. The positive entropy change, shown by the red regions in Fig. 4(a)-(c), is found for all three types of skyrmions realized in

our two-dimensional systems, and also observed in three-dimensional materials in experiments [6, 8, 9].

Spin fluctuations play an important role in the temperature-driven phase transitions in Dzyaloshinskii-Moriya magnets [36]. Magnetic entropy change, obtained via measurements of magnetization and specific heat, can provide a great amount of information about the nature of the fluctuation-dominated phase transitions [6, 37, 38]. Both experimental and theoretical studies suggest that the temperature-driven transition from the paramagnetic to the SkX phase occurs via a precursor phase in which non-trivial topological spin textures of skyrmionic character are developed within a paramagnetic background with abundance of fluctuations [20, 22, 39]. This is evident from the plots of the skyrmion number N_{sk} in Fig. 4(d)-(f), as this number fluctuates and its non-zero value is extended up to much higher temperature above the SkX phase, which prevails at temperatures $T \lesssim 1.5J$. This fluctuation-dominated weak first order phase transition, also known as the Brazovskii transition, exists also at higher fields, as it can be seen from the magnetic entropy change in going from the paramagnetic to the ferromagnetic phase. The results presented in Fig. 3 and Fig. 4 enable us to conclude that the precursor phase involving skyrmions exists at temperatures $T \lesssim 3J$, below which ΔS_m changes its slope. The essential features of

ΔS_m are qualitatively the same for all three types of DMI considered in our models.

IV. DISCUSSION AND SUMMARY

Because of the sign reversal in the magnetic entropy change ΔS_m in the SkX phase, the fractional change in the magnetic entropy in transitioning from the fully-polarized FM phase to the SkX phase *i.e.* $|\Delta S_m^{\text{SkX}} - \Delta S_m^{\text{FM}}|/\Delta S_m^{\text{FM}}$ is always larger than the fractional change in the magnetic entropy in transitioning from the PM phase to the FM phase *i.e.* $|\Delta S_m^{\text{FM}} - \Delta S_m^{\text{PM}}|/\Delta S_m^{\text{PM}}$. In Fig. 5(a), the two routes for magnetic cooling process are shown; the PM to FM path is used in conventional magnetic cooling methods based on the magnetocaloric effect (MCE). The phase boundaries can be drawn explicitly by using various observables such as magnetization, spin-spin correlation function, skyrmion number and topological Hall conductivity, as done in previous studies [17, 40]. The MCE also depends significantly on the nature of the variation in magnetization near the phase transitions. Based on the nature of the magnetic transition, a variety of magnetic materials have been proposed to enhance the efficiency of the MCE [41]. Materials with a first-order phase transition to the magnetically-ordered phase exhibit a large change in the magnetization over a small temperature range. It results in an abrupt change in the magnetic entropy, which leads to losses by hysteresis and irreversibilities of the magnetic state during demagnetization [42]. The energy lost during the cycle involving the magnetization and demagnetization, is dissipated as heat via the magnetic circuits. Since the Maxwell's relation in Eq. (1) is valid for systems in equilibrium, the dissipative kinetics essentially reduces the efficiency of the MCE of these materials. Additional structural transitions have also been reported in the vicinity of the first-order magnetic phase transition [43]. Materials with a smooth phase transition to the magnetically-ordered phase are, on the other hand, free from these penalizing phenomena such as hysteresis loss, slow kinetics and structural transition. Because of the above advantages, we propose materials hosting the SkX phase to be good candidates for the magnetocaloric applications. A typical cycle of the magnetic cooling method involving a SkX phase and a FM phase is shown in Fig. 5(b). The proposed refrigeration cycle is performed by adiabatically magnetizing the system to FM phase from SkX phase, causing magnetic heating. This heat is then expelled through the system which again undergoes magnetic cooling through adiabatic demagnetization. Finally, the system absorbs heat from the environment and reaches its thermal equilibrium, from which it can restart the magnetic refrigeration cycle.

To summarize, we investigated the magnetic entropy change in two-dimensional magnets hosting various kinds of skyrmion crystals and the nature of fluctuation-dominated phase transitions. Our results confirm sev-

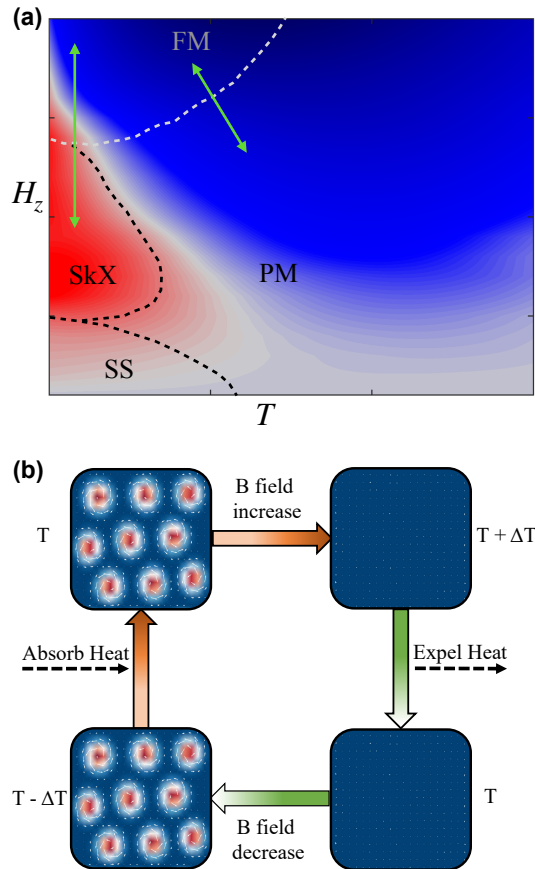


FIG. 5. (a) Schematic phase diagram, showing two routes of phase transition (green arrows) for magnetic cooling cycle: one between the paramagnetic (PM) and ferromagnetic (FM) phases, and another between the skyrmion crystal (SkX) and the FM phases. (b) Proposed cooling cycle between the SkX and the FM phases. Increasing magnetic field causes FM ordering, which results in increase in temperature of the material. Once excess heat is expelled out, the material is again demagnetized, and the temperature is decreased.

eral experimental reports and suggest that the magnetic entropy change can be used as a general probe, as an useful alternative to neutron probes in momentum space [1, 22, 44], transmission-electron microscopy imaging in real space [45–47] or topological Hall effect-based probes [11, 12, 15, 16], to analyze the nature of phase transitions in Dzyaloshinskii-Moriya magnets in two and three dimensions. Our study also provides interesting perspectives about magnetocaloric effect in the SkX phase, and suggest that magnetic materials which host the SkX phase can be used in efficient magnetic cooling applications. More stable topological magnetic phases, such as hopfions which appear in three-dimensional materials, open up a new path towards the exploration of magnetocaloric applications with enhanced efficiency at elevated temperatures [48–50].

ACKNOWLEDGEMENTS

NM acknowledges support of an initiation grant (No. IITR/SRIC/2116/FIG) from IIT Roorkee and SRG grant (No. SRG/2023/001188) from SERB. Numerical calculations were performed at the computing resources of

PARAM Ganga at IIT Roorkee, provided by National Supercomputing Mission, implemented by C-DAC, and supported by the Ministry of Electronics and Information Technology and Department of Science and Technology, Government of India.

-
- [1] C. Pappas, E. Lelièvre-Berna, P. Falus, P. M. Bentley, E. Moskvina, S. Grigoriev, P. Fouquet, and B. Farago, “Chiral paramagnetic skyrmion-like phase in MnSi,” *Phys. Rev. Lett.* **102**, 197202 (2009).
 - [2] E. Ruff, P. Lunkenheimer, A. Loidl, H. Berger, and S. Krohns, “Magnetoelectric effects in the skyrmion host material Cu_2OSeO_3 ,” *Sci. Rep.* **5**, 15025 (2015).
 - [3] Pardeep, Lalita, Y. Bitla, S. Saha, A. K. Patra, and G. A. Basheed, “Chiral-fluctuations mediated helical to paramagnetic phase transition and scaling study in β -Mn type $\text{Co}_8\text{Zn}_8\text{Mn}_4$ chiral magnet,” *J. Phys.: Condens. Matter* **35**, 175801 (2023).
 - [4] M. Ge, L. Zhang, D. Menzel, H. Han, C. Jin, C. Zhang, L. Pi, and Y. Zhang, “Scaling investigation of the magnetic entropy change in helimagnet MnSi,” *J. Alloys Compd.* **649**, 46 (2015).
 - [5] H. Han, D. Menzel, W. Liu, L. Ling, H. Du, L. Pi, C. Zhang, L. Zhang, and Y. Zhang, “Scaling of the magnetic entropy change in skyrmion material $\text{Fe}_{0.5}\text{Co}_{0.5}\text{Si}$,” *Mater. Res. Bull.* **94**, 500 (2017).
 - [6] J. D. Bocarsly, R. F. Need, R. Seshadri, and S. D. Wilson, “Magnetotransport signatures of skyrmionic phase behavior in FeGe,” *Phys. Rev. B* **97**, 100404 (2018).
 - [7] S. Jamaluddin, S. K. Manna, B. Giri, P. V. P. Madduri, S. S. P. Parkin, and A. K. Nayak, “Robust anti-skyrmion phase in bulk tetragonal Mn-Pt(Pd)-Sn heusler system probed by magnetic entropy change and AC-susceptibility measurements,” *Adv. Funct. Mater.* **29**, 1901776 (2019).
 - [8] C. Dhital and J. F. DiTusa, “Entropic signatures of the skyrmion lattice phase in $\text{MnSi}_{1-x}\text{Al}_x$ and $\text{Fe}_{1-y}\text{Co}_y\text{Si}$,” *Phys. Rev. B* **102**, 224408 (2020).
 - [9] J. L. Zuo, D. Kitchaev, E. C. Schueller, J. D. Bocarsly, R. Seshadri, A. Van der Ven, and S. D. Wilson, “Magnetotransport mapping and computational modeling of cycloids and skyrmions in the lacunar spinels GaV_4S_8 and GaV_4Se_8 ,” *Phys. Rev. Mater.* **5**, 054410 (2021).
 - [10] X. Li, W. V. Liu, and L. Balents, “Spirals and skyrmions in two dimensional oxide heterostructures,” *Phys. Rev. Lett.* **112**, 067202 (2014).
 - [11] T. Yokouchi, N. Kanazawa, A. Tsukazaki, Y. Kozuka, A. Kikkawa, Y. Taguchi, M. Kawasaki, M. Ichikawa, F. Kagawa, and Y. Tokura, “Formation of in-plane skyrmions in epitaxial MnSi thin films as revealed by planar Hall effect,” *J. Phys. Soc. Japan* **84**, 104708 (2015).
 - [12] J. Matsuno, N. Ogawa, K. Yasuda, F. Kagawa, W. Koshibae, N. Nagaosa, Y. Tokura, and M. Kawasaki, “Interface-driven topological Hall effect in SrRuO_3 - SrIrO_3 bilayer,” *Sci. Adv.* **2**, e1600304 (2016).
 - [13] J. Rowland, S. Banerjee, and M. Randeria, “Skyrmions in chiral magnets with Rashba and Dresselhaus spin-orbit coupling,” *Phys. Rev. B* **93**, 020404 (2016).
 - [14] M. Hoffmann, B. Zimmermann, G. P. Muller, D. Schurhoff, N. S. Kiselev, C. Melcher, and S. Blugel, “Antiskyrmions stabilized at interfaces by anisotropic Dzyaloshinskii-Moriya interactions,” *Nat. Commun.* **8**, 308 (2017).
 - [15] M. Nakamura, D. Morikawa, X. Yu, F. Kagawa, T. Arima, Y. Tokura, and M. Kawasaki, “Emergence of topological Hall effect in half-metallic manganite thin films by tuning perpendicular magnetic anisotropy,” *J. Phys. Soc. Japan* **87**, 074704 (2018).
 - [16] L. Vistoli, W. Wang, A. Sander, Q. Zhu, B. Casals, R. Cicheler, A. Barthélémy, S. Fusil, G. Herranz, S. Valencia, R. Abrudan, E. Weschke, K. Nakazawa, H. Kohno, J. Santamaria, W. Wu, V. Garcia, and M. Bibes, “Giant topological Hall effect in correlated oxide thin films,” *Nat. Phys.* **15**, 67 (2019).
 - [17] N. Mohanta, E. Dagotto, and S. Okamoto, “Topological Hall effect and emergent skyrmion crystal at manganite-iridate oxide interfaces,” *Phys. Rev. B* **100**, 064429 (2019).
 - [18] T.-E. Park, L. Peng, J. Liang, A. Hallal, F. S. Yasin, X. Zhang, K. M. Song, S. J. Kim, K. Kim, M. Weigand, G. Schütz, S. Finizio, J. Raabe, K. Garcia, J. Xia, Y. Zhou, M. Ezawa, X. Liu, J. Chang, H. C. Koo, Y. D. Kim, M. Chshiev, A. Fert, H. Yang, X. Yu, and S. Woo, “Néel-type skyrmions and their current-induced motion in van der Waals ferromagnet-based heterostructures,” *Phys. Rev. B* **103**, 104410 (2021).
 - [19] A. Bauer, M. Garst, and C. Pfleiderer, “Specific heat of the skyrmion lattice phase and field-induced tricritical point in MnSi,” *Phys. Rev. Lett.* **110**, 177207 (2013).
 - [20] H. Wilhelm, M. Baenitz, M. Schmidt, U. K. Rossler, A. A. Leonov, and A. N. Bogdanov, “Precursor phenomena at the magnetic ordering of the cubic helimagnet FeGe,” *Phys. Rev. Lett.* **107**, 127203 (2011).
 - [21] S. Shanmukharao Samatham and V. Ganesan, “Precursor state of skyrmions in MnSi: A heat capacity study,” *Phys. Status Solidi* **7**, 184 (2013).
 - [22] J. Kindervater, I. Stasinopoulos, A. Bauer, F. X. Haslbeck, F. Rucker, A. Chacon, S. Mühlbauer, C. Franz, M. Garst, D. Grundler, and C. Pfleiderer, “Weak crystallization of fluctuating skyrmion textures in MnSi,” *Phys. Rev. X* **9**, 041059 (2019).
 - [23] L. Caron, Z.Q. Ou, T.T. Nguyen, D.T. Cam Thanh, O. Tegus, and E. Bruck, “On the determination of the magnetic entropy change in materials with first-order transitions,” *J. Magn. Magn. Mater.* **321**, 3559 (2009).
 - [24] J. Wild, T. N. G. Meier, S. Pollath, M. Kronseder, A. Bauer, A. Chacon, M. Halder, M. Schowalter, A. Rosenauer, J. Zweck, J. Muller, A. Rosch, C. Pfleiderer, and C. H. Back, “Entropy-limited topological protection of skyrmions,” *Sci. Adv.* **3**, e1701704 (2017).

- [25] L. Caron, Z.Q. Ou, T.T. Nguyen, D.T. Cam Thanh, O. Tegus, and E. Bruck, “On the determination of the magnetic entropy change in materials with first-order transitions,” *J. Magn. Magn. Mater.* **321**, 3559 (2009).
- [26] J. S. Amaral and V. S. Amaral, “The effect of magnetic irreversibility on estimating the magnetocaloric effect from magnetization measurements,” *Appl. Phys. Lett.* **94**, 042506 (2009).
- [27] M. Balli, D. Fruchart, D. Gignoux, and R. Zach, “The colossal magnetocaloric effect in $\text{Mn}_{1-x}\text{Fe}_x\text{As}$: What are we really measuring,” *Appl. Phys. Lett.* **95**, 072509 (2009).
- [28] A. Magnus G. Carvalho, A.A. Coelho, P.J. von Ranke, and C.S. Alves, “The isothermal variation of the entropy (δst) may be miscalculated from magnetization isotherms in some cases: MnAs and $\text{Gd}_5\text{Ge}_2\text{Si}_2$ compounds as examples,” *J. Alloys Compd.* **509**, 3452 (2011).
- [29] A. Bogdanov and A. Hubert, “The stability of vortex-like structures in uniaxial ferromagnets,” *J. Magn. Magn. Mater.* **195**, 182 (1999).
- [30] S. Banerjee, J. Rowland, O. Erten, and M. Randeria, “Enhanced stability of skyrmions in two-dimensional chiral magnets with Rashba spin-orbit coupling,” *Phys. Rev. X* **4**, 031045 (2014).
- [31] U. Gungordu, R. Nepal, O. A. Tretiakov, K. Belashchenko, and A. A. Kovalev, “Stability of skyrmion lattices and symmetries of quasi-two-dimensional chiral magnets,” *Phys. Rev. B* **93**, 064428 (2016).
- [32] A. O. Leonov and I. Kezsmarki, “Skyrmion robustness in noncentrosymmetric magnets with axial symmetry: The role of anisotropy and tilted magnetic fields,” *Phys. Rev. B* **96**, 214413 (2017).
- [33] R. Ozawa, S. Hayami, and Y. Motome, “Zero-field skyrmions with a high topological number in itinerant magnets,” *Phys. Rev. Lett.* **118**, 147205 (2017).
- [34] S. Hayami and Y. Motome, “Square skyrmion crystal in centrosymmetric itinerant magnets,” *Phys. Rev. B* **103**, 024439 (2021).
- [35] N. Mohanta and E. Dagotto, “Interfacial phase frustration stabilizes unconventional skyrmion crystals,” *npj Quantum Mater.* **7**, 76 (2022).
- [36] M. Janoschek, M. Garst, A. Bauer, P. Krautscheid, R. Georgii, P. Boni, and C. Pfleiderer, “Fluctuation-induced first-order phase transition in Dzyaloshinskii-Moriya helimagnets,” *Phys. Rev. B* **87**, 134407 (2013).
- [37] L. Kautzsch, J. D. Bocarsly, C. Felser, S. D. Wilson, and R. Seshadri, “Controlling Dzyaloshinskii-Moriya interactions in the skyrmion host candidates $\text{FePd}_{1-x}\text{Pt}_x\text{Mo}_3\text{N}$,” *Phys. Rev. Mater.* **4**, 024412 (2020).
- [38] E. C. Schueller, D. A. Kitchaev, J. L. Zuo, J. D. Bocarsly, J. A. Cooley, A. Van der Ven, S. D. Wilson, and R. Seshadri, “Structural evolution and skyrmionic phase diagram of the lacunar spinel GaMo_4Se_8 ,” *Phys. Rev. Mater.* **4**, 064402 (2020).
- [39] N. Mohanta, A. D. Christianson, S. Okamoto, and E. Dagotto, “Signatures of a liquid-crystal transition in spin-wave excitations of skyrmions,” *Commun. Phys.* **3**, 229 (2020).
- [40] N. Mohanta, S. Okamoto, and E. Dagotto, “Planar topological Hall effect from conical spin spirals,” *Phys. Rev. B* **102**, 064430 (2020).
- [41] V. Franco, J.S. Blázquez, B. Ingale, and A. Conde, “The magnetocaloric effect and magnetic refrigeration near room temperature: Materials and models,” *Annu. Rev. Mater. Res.* **42** (2012).
- [42] S. Mellari, “Introduction to magnetic refrigeration: magnetocaloric materials,” *Int. J. Air-Cond. Refrig.* **31**, 5 (2023).
- [43] A. Murtaza, W. Zuo, M. Yaseen, A. Ghani, A. Saeed, C. Hao, J. Mi, Y. Li, T. Chang, L. Wang, C. Zhou, Y. Wang, Y. Zhang, S. Yang, and Y. Ren, “Magnetocaloric effect in the vicinity of the magnetic phase transition in $\text{NdCo}_{2-x}\text{Fe}_x$ compounds,” *Phys. Rev. B* **101**, 214427 (2020).
- [44] S. Mühlbauer, B. Binz, F. Jonietz, C. Pfleiderer, A. Rosch, A. Neubauer, R. Georgii, and P. Boni, “Skyrmion lattice in a chiral magnet,” *Science* **323**, 915 (2009).
- [45] X. Z. Yu, Y. Onose, N. Kanazawa, J. H. Park, J. H. Han, Y. Matsui, N. Nagaosa, and Y. Tokura, “Real-space observation of a two-dimensional skyrmion crystal,” *Nature* **465**, 901 (2010).
- [46] X. Z. Yu, N. Kanazawa, Y. Onose, K. Kimoto, W. Z. Zhang, S. Ishiwata, Y. Matsui, and Y. Tokura, “Near room-temperature formation of a skyrmion crystal in thin-films of the helimagnet FeGe ,” *Nat. Mater.* **10**, 106 (2011).
- [47] Y. Tokunaga, X. Z. Yu, J. S. White, H. M. Ronnow, D. Morikawa, Y. Taguchi, and Y. Tokura, “A new class of chiral materials hosting magnetic skyrmions beyond room temperature,” *Nat. Commun.* **6**, 7638 (2015).
- [48] Y. Tokunaga, X. Z. Yu, J. S. White, H. M. Ronnow, D. Morikawa, Y. Taguchi, and Y. Tokura, “A new class of chiral materials hosting magnetic skyrmions beyond room temperature,” *Nat. Commun.* **6**, 7638 (2015).
- [49] N. Kent, N. Reynolds, D. Raftrey, I. T. G. Campbell, S. Virasawmy, S. Dhuey, R. V. Chopdekar, A. Hierro-Rodriguez, A. Sorrentino, E. Pereiro, S. Ferrer, F. Hellman, P. Sutcliffe, and P. Fischer, “Creation and observation of Hopfions in magnetic multilayer systems,” *Nat. Commun.* **12**, 1562 (2021).
- [50] F. N. Rybakov, N. S. Kiselev, A. B. Borisov, L. Doring, C. Melcher, and S. Blugel, “Magnetic hopfions in solids,” *APL Mater.* **10**, 111113 (2022).